Inorganic Chemistry

Article

pubs.acs.org/IC

The 16 $CB_{11}(CH_3)_n(CD_3)_{12-n}^{\bullet}$ Radicals with 5-Fold Substitution Symmetry: Spin Density Distribution in $CB_{11}Me_{12}^{\bullet}$

Jiří Kaleta,[†] Ján Tarábek,[†] Akin Akdag,[†,‡] Radek Pohl,[†] and Josef Michl*[,†,‡]

[†]Institute of Organic Chemistry and Biochemistry, Academy of Sciences of the Czech Republic, Flemingovo nám. 2, 16610 Prague, Czech Republic

[‡]Department of Chemistry and Biochemistry, University of Colorado, Boulder, Colorado 80309-0215, United States

Supporting Information

ABSTRACT: The syntheses of all 16 $CB_{11}(CH_3)_n(CD_3)_{12-n}^{\bullet}$ radicals with 5-fold substitution symmetry are described. The variation in the width of their broad and featureless electron paramagnetic resonance signals as a function of the deuteriation pattern is used to deduce the relative values of the average hyperfine coupling constants a_H of the hydrogen atoms in the ipso (1), ortho (2−6), meta (7−11), and para (12) methyl groups, $a_H(i):a_H(o):a_H(m):a_H(p)$ = (0.18 ± 0.09):(0.71 ± 0.02):(1.00 ± 0.03):(0.52 ± 0.05), and these can be compared with ratios expected from a B3LYP/EPRII calculation, 0.04:0.55:1:0.51.

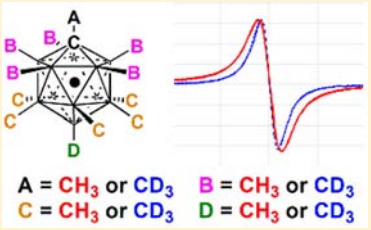

INTRODUCTION

The study of carboranes has flourished for decades and recently has been finding applications in other areas of chemistry.[1] The icosahedral monocarba-*closo*-dodecaborane clusters CB_{11}^{-}[2] have been investigated in particular detail, owing to the advantages that their highly stable closed-shell anions offer as inert counterions in work with unusually electrophilic cations: low nucleophilicity and basicity and resistance to oxidation.[3] The low nucleophilicity of the anions,[4] the extreme Brønsted acidity of their conjugate acids,[5−7] and the remarkable Lewis acidity of their lithium salts[8,9] have already been explored to some extent. The high redox potentials of the $CB_{11}^{-}/CB_{11}^{\bullet}$ redox couples have also started to receive attention.[10−14] Quantitative work is hindered, in part, by the instability of the parent $CB_{11}H_{12}^{\bullet}$ and similar deltahedral radicals[12,15−20] toward dimerization and, in part, by their strongly oxidizing nature, which limits the choice of solvents.[13] It has gradually become clear that dimerization can be suppressed by steric hindrance by inert substituents in positions 7−12.[11,12,14] Nearly two dozen stable and chemically reversible redox couples derived from the substituted icosahedral clusters $CB_{11}^{-}/CB_{11}^{\bullet}$ are now known.[14] Such couples might be interesting for applications in photovoltaics and batteries.

Only one of the electroneutral free radicals, $CB_{11}Me_{12}^{\bullet}$, has, however, been isolated and characterized structurally and spectroscopically,[11] although the colors and spectra of some others have been observed in solution.[13] The electron paramagnetic resonance (EPR) spectrum of $CB_{11}Me_{12}^{\bullet}$ consists of a single broad, featureless, and uninformative peak, which suggests that the spin density is distributed over most or all of the 11 boron atoms present in their natural isotopic abundance. An attempt to obtain an ENDOR spectrum failed because the EPR signal could not be saturated even at the lowest temperatures,[11] and nothing is known about the hyperfine coupling constants and the distribution of spin density in the molecule.

The chemical reactivity of $CB_{11}Me_{12}^{\bullet}$ is understood better. This radical acts as a strong one-electron oxidant[11,21,22] and as an agent that transfers a methyl radical to disilanes[23] and to alkenes,[24] but it is not known with certainty which of its many methyls is transferred. The methyl radical transfer reaction is analogous to the methyl anion transfer reactions postulated for the action of strong Lewis acids on anions of the type $CB_{11}Me_{12}^{-}$,[25] where there also is some uncertainty as to which methyl groups are involved.

The objective of the present paper is to deduce information about the hyperfine coupling constants a_H in $CB_{11}Me_{12}^{\bullet}$, at least approximately, in spite of the discouraging appearance of its EPR signal. The experimental procedure used is general and might be useful for other radicals with unresolved and uninformative EPR spectra.

RESULTS

Synthesis of Anions $CB_{11}(CH_3)_n(CD_3)_{12-n}^{-}$. The preparation of the cesium salts of the 16 anions **1**−**16** (Chart 1) made use of the strategies employed previously[12] for the synthesis of the 16 symmetric anions $CB_{11}H_n(CH_3)_{12-n}^{-}$ (Schemes 1 and 2). The reactions used were those listed in Scheme 2 of ref 12 [deprotonation followed by methylation or tri(isopropyl)-silylation at the carbon vertex, methylation at boron vertices with methyl triflate, iodination with ICl or I_2, desilylation with CsF, and protodeiodination under Birch conditions]. The replacement of an iodine substituent with a methyl group was not performed using a Kumada reaction as before but using $AlMe_3$.[26] In several cases, the synthesis and isolation of the intermediates and the final products were improved.

Received: June 10, 2012
Published: September 20, 2012

 © 2012 American Chemical Society dx.doi.org/10.1021/ic301236s | *Inorg. Chem.* 2012, 51, 10819−10824

Chart 1. Structures of Symmetrically Deuteriated Dodecamethylcarborate Anions (1−16; ★ = −) and Radicals (1r−16r; ★ = •)

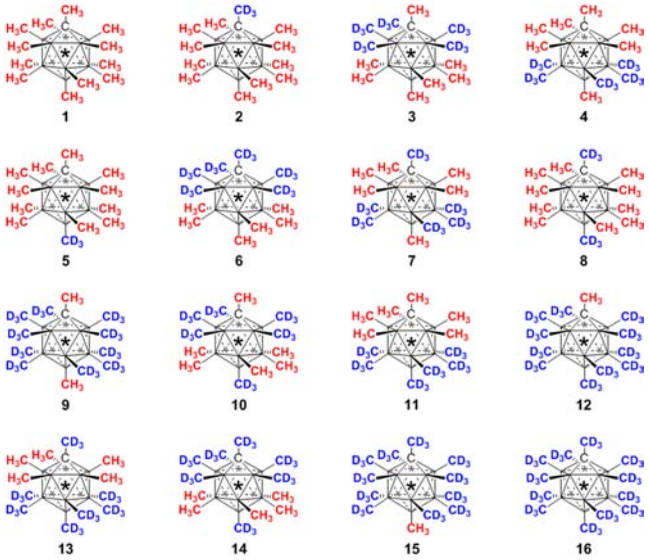

Unexpectedly, the attempted introduction of CD_3 groups on BH vertices by the action of $TfOCD_3$ in sulfolane yields a mixture of CD_3 and CHD_2 substituted products, as revealed by NMR and IR spectra. The exact content of deuterium in each of the four distinct types of position in the anions **1**−**16** was determined by NMR. There is no indication of the formation of CH_2D or CH_3 substituents in this reaction. It appears that the hydrogen atom initially present on the BH vertex can scramble with the deuterium atoms of the CD_3 group. We have investigated this process computationally and will report the results separately.

Preparation of Radicals $CB_{11}(CH_3)_n(CD_3)_{12-n}^{\bullet}$. The radicals **1r**−**16r** were prepared by oxidation of the anions with PbO_2/CF_3COOH and extraction into pentane, as reported for the undeuteriated parent.[11] The pentane solutions were used directly for EPR measurements.

Hyperfine Coupling Constants. Room-temperature EPR spectra of all 16 radicals were similar and contained a single broad line at g = 2.0046 ± 0.0002, in agreement with the previous report.[11] The spectra obtained in frozen pentane at 77 K were similar but somewhat broader (g = 2.0053 ± 0.0002). The spectra of **1r** and **16r** are shown in Figure 1 as examples.

The derivative EPR spectral curves could not be fitted to Gaussian or Lorentzian derivative shapes. Their width was characterized by the positive-to-negative peak distance B_1 and by the distances $B_{1/n}$ between the points at which the derivative spectral curve amplitude is reduced by the factor n from the value at maximum positive and negative peaks. This is a generalization of the commonly used full width at a half-maximum $B_{1/2}$ (Tables 1 and S3 in the Supporting Information, part C). In order to evaluate the relative magnitudes of the hyperfine splitting constants a_H and a_D (equal to $0.153a_H$) from the observed spectra, the following assumptions were made: (i) The coupling constants for all hydrogen atoms within a methyl group are equal. This is justified if methyl rotation is fast on the EPR time scale. (ii) There are no isotope effects on the structure or spin densities. This is a common approximation. (iii) The coupling constants for all methyl groups that are symmetry-equivalent in the anion are equal. This is justified if the Jahn−Teller distortion from 5-fold symmetry in the radical is dynamic and fast on the EPR time scale. The very fast spin relaxation that is observed even at the lowest temperatures and

Scheme 1. Synthesis of Anions 1, 2, 5, 8, 9, 12, 15, and 16[a]

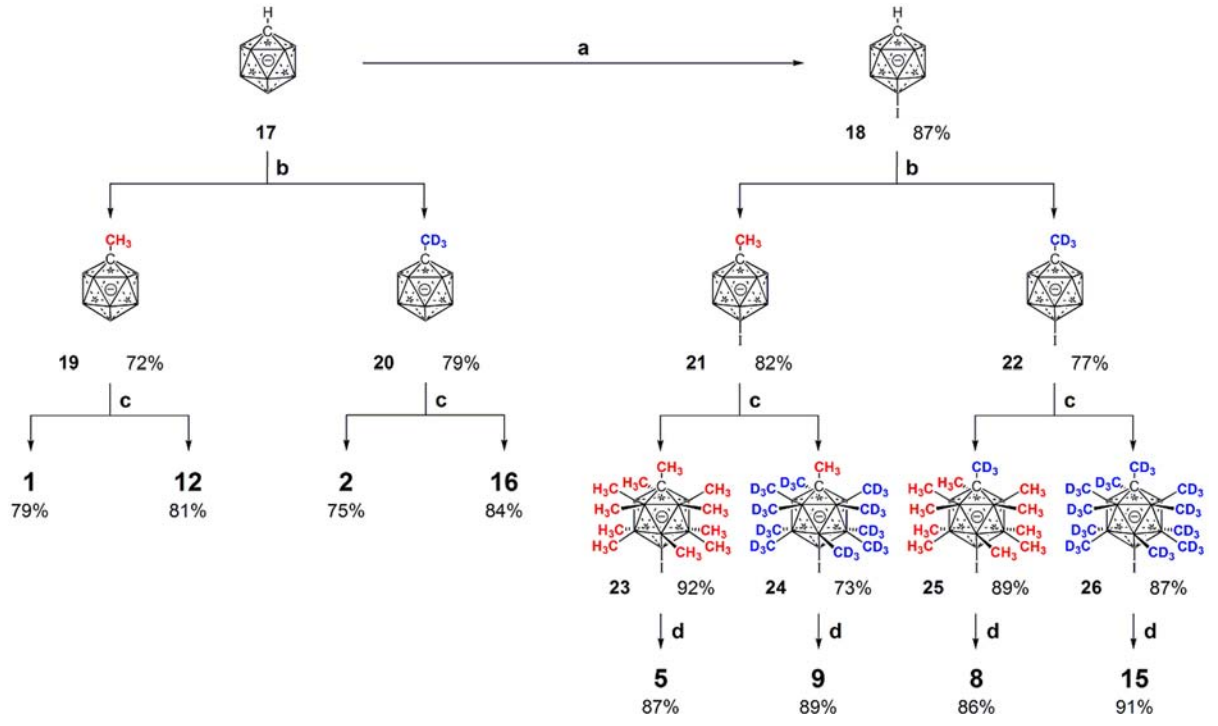

[a](a) I_2, CH_3COOH, 40 °C. (b) 1. *n*-BuLi, THF/hexane, −78 °C → 25 °C. 2. CH_3I or CD_3I, THF/hexane, −78 °C → 25 °C. (c) $TfOCH_3$ or $TfOCD_3$, CaH_2, sulfolane, 25 °C. (d) $Al(CH_3)_3$ or $Al(CD_3)_3$, toluene, 135 °C.

dx.doi.org/10.1021/ic301236s | *Inorg. Chem.* 2012, 51, 10819−10824

Scheme 2. Synthesis of Anions 3, 4, 6, 7, 10, 11, 13, and 14[a]

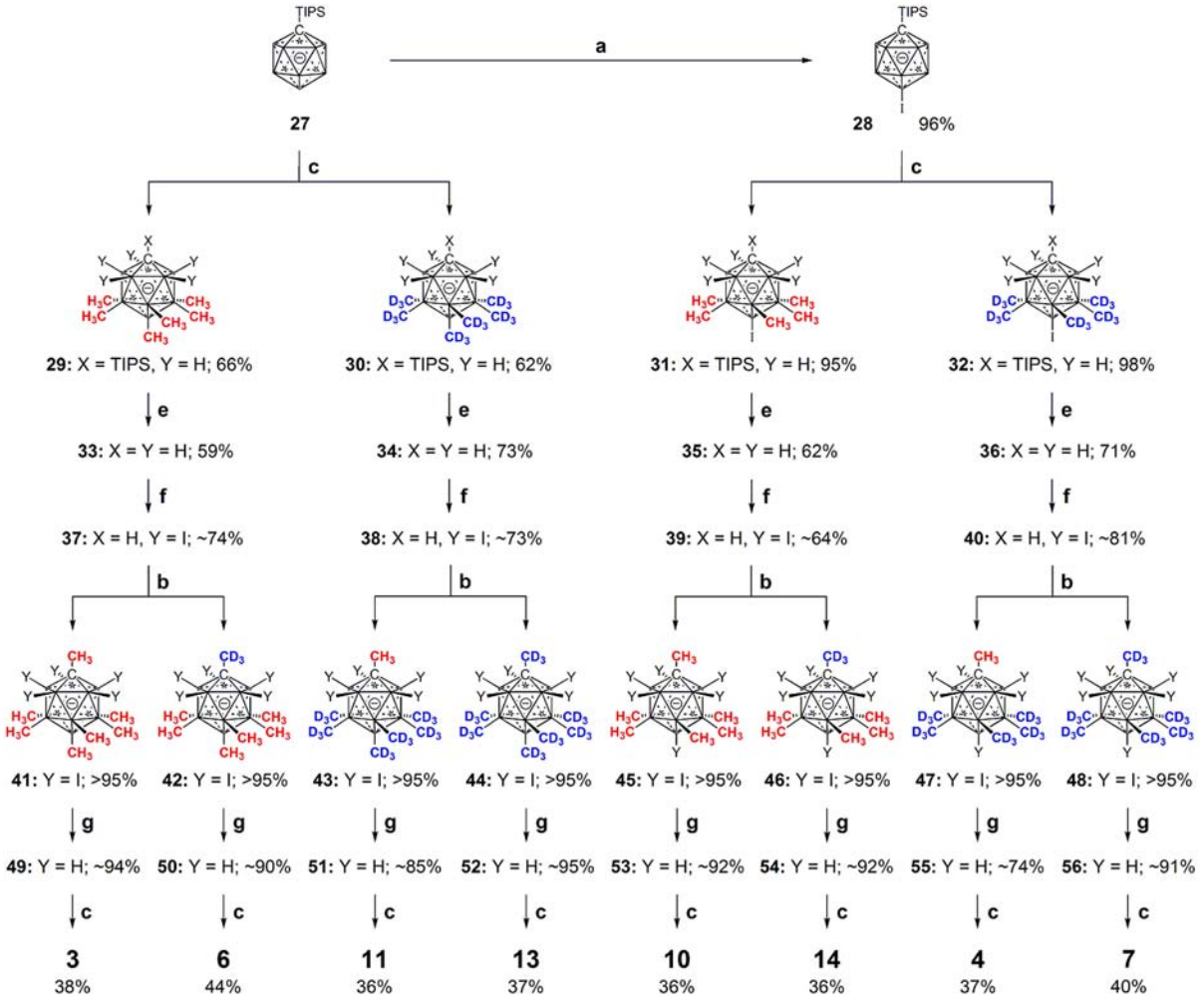

[a](a) I_2, CH_3COOH, 40 °C. (b) 1. *n*-BuLi, THF/hexane, −78 °C → 25 °C. 2. CH_3I or CD_3I, THF/hexane, −78 °C → 25 °C. (c) $TfOCH_3$ or $TfOCD_3$, CaH_2, sulfolane, 25 °C. (e) 1. CsF, sulfolane, 190 °C. 2. H_2O, 25 °C. (f) ICl, 1,1,2,2-tetrachloroethane/1,2-dimethoxyethane, 150 °C. (g) $Na/NH_3(l)$, −78 °C.

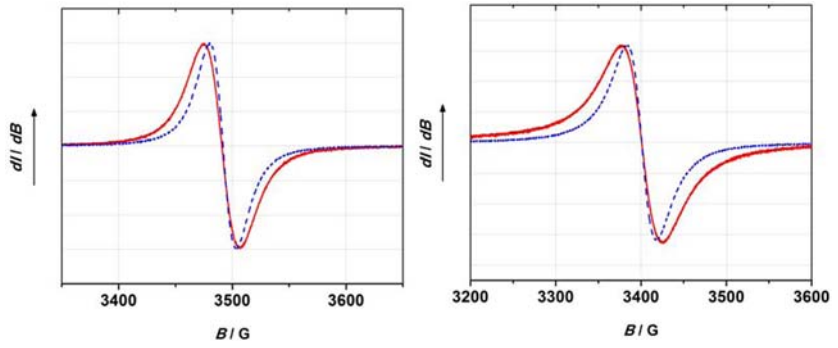

Figure 1. Derivative EPR spectra of **1r** (solid red line) and **16r** (dashed blue line) in pentane at (left) 293 and (right) 77 K.

that prevents signal saturation and thus also ENDOR measurements is compatible with such fast Jahn−Teller dynamics. Assumptions (i)−(iii) simplify analysis of the EPR spectrum by reducing the number of distinct a_H constants to four: $a_H(i)$ for the hydrogen atoms of a methyl located in the ipso position 1, $a_H(o)$ for the ortho positions 2−6, $a_H(m)$ for the meta positions 7−11, and $a_H(p)$ for the para position 12.

An additional assumption is needed because the large number of ^{10}B (20% abundance, spin 3), ^{11}B (80% abundance, spin $^3/_2$), ^1H (~100% abundance, spin $^1/_2$), and ^{13}C (1% abundance, spin $^1/_2$) atoms in the four distinct positions of the cage causes the number of EPR lines to be too huge to be distinguished individually, especially given the likely dynamic broadening, and because the measurement of ENDOR failed. We note that the inobservable overall width of the isotropic

dx.doi.org/10.1021/ic301236s | *Inorg. Chem.* 2012, 51, 10819−10824

Table 1. Room-Temperature Line Widths $B_{1/n}$/G in EPR Spectra of 1r and 16r in Pentane for Selected Values of n (See Also Table S3 in the Supporting Information)

	n				
radical	1	$^4/_3$	2	4	10
1r	31.7	52.8	68.9	93	129
16r	22.1	39.5	52.7	73	106
$\lvert\delta(B_{1/n})\rvert$/G	0.4	0.5	0.8	1	1

liquid solution spectrum (outer line to outer line distance) is equal to the sum of all coupling constants of the nuclei present and assume (iv) that the line widths $B_{1/n}$ are proportional to the sum of all coupling constants.

Given assumptions (i)−(iii), replacement of hydrogen with deuterium in a methyl group located in a particular position α ($\alpha = i$, o, m, or p) will replace its contribution $a_H(\alpha)$ to the total spectral width with the contribution a_D and thus reduce it by a factor of 0.153. According to assumption (iv), it will therefore reduce the line widths $B_{1/n}$. This leads us to define additive line-narrowing increments $ka_H(\alpha)$, with $\alpha = i$, o, m, or p, where k is an unknown proportionality constant, different for each value of n chosen in the line-width evaluation. The constant k is related to the unknown fraction of the total line width that is due to hyperfine coupling with protons. To derive the $ka_H(\alpha)$ increments from the differences $\Delta B^j_{1/n}$ of the line widths $B^j_{1/n}$ observed in the spectra of the deuteriated radicals **2r−16r** (**jr**, j = 2−16) and that observed in the spectrum of the fully protiated radical **1r** (Table 1), we used a least-squares solution of the overdetermined set of 15 equations for four unknowns for each value of n (see the Supporting Information for details):

$$k_{1/n}\sum_\alpha a_H(\alpha)\,N^j(\alpha) = \Delta B^j{}_{1/n},$$
$$\alpha = i,\ o,\ m,\ p \text{ and } j = 2-16 \qquad (1)$$

The values of the line-narrowing increments $ka_H(\alpha)$ and the coupling constant ratios were obtained for 17 choices of n ranging from 1 to $^{57}/_4$, and several are shown in Table 2 (see also Table S2 in the Supporting Information, part C). The least-squares fits are excellent for all choices of n and support the assumption of additive increments. An example (n = 1) of the correlation between the values $\Delta B^j{}_{1/n}{}^{\text{incr}} = k_{1/n}\sum_\alpha a_H(\alpha)\,N^j(\alpha)$ obtained from the increments and the measured values $\Delta B^j{}_{1/n}$ is shown in Figure 2. The regression line is

$$\Delta B^j{}_1{}^{\text{incr}} = (1.01 \pm 0.02)\Delta B^j{}_1 + (0.0 \pm 0.2),\quad r = 0.999 \qquad (2)$$

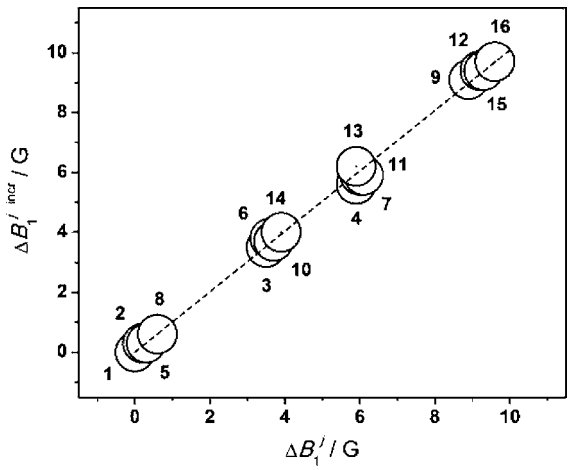

Figure 2. Peak-to-peak EPR line narrowing relative to **1r** (j = 1), calculated from line-narrowing increments ($\Delta B^j{}_1{}^{\text{incr}}$) and observed ($\Delta B^j{}_1$), for j = 2−16.

The results obtained for the 17 choices of n are similar and do not show systematic trends. The average values given in the last column of Table 2 provide our best approximation to the relative values of the hyperfine coupling constants.

Calculations. Hyperfine constants $a_H(\alpha)$ in **1r** were calculated at a M06-2X/cc-pVTZ-optimized geometry using the B3LYP/EPRII method (see the Supporting Information, part C). Values averaged within each methyl group and over all methyl groups that are symmetry equivalent in the anion are shown in Table 2 for comparison with the experimentally derived line-narrowing increments. Table 3 shows the

Table 3. B3LYP/EPRII-Calculated Spin Densities σ

α	$\sigma_H(\alpha)$	$\sigma_{Me}(\alpha)$	$\sigma_{RMe}(\alpha)^a$
ipso	0.0008	0.0011	−0.0076
ortho	0.0504	0.0800	0.3195
meta	0.0845	0.1513	0.6249
para	0.0079	0.0095	0.0632

[a] R = C when α = ipso; R = B otherwise.

Table 2. EPR Line-Narrowing Increments $k_{1/n}a_H(\alpha)$/G and Ratios $a_H(\alpha)/a_H(m)$ for Selected Values of n and B3LYP/EPRII Calculated Hyperfine Coupling Constants a_H^{DFT}

	$k_{1/n}a_H(\alpha)$, where n =						
α	1	$^4/_3$	2	4	10	ave[b]	a_H^{DFT}/G[a]
i	0.06 ± 0.11	0.03 ± 0.12	0.26 ± 0.19	0.28 ± 0.24	0.30 ± 0.24		0.2
o	0.29 ± 0.03	0.46 ± 0.03	0.54 ± 0.05	0.66 ± 0.06	0.83 ± 0.06		2.6
m	0.45 ± 0.03	0.60 ± 0.03	0.75 ± 0.05	0.95 ± 0.07	1.04 ± 0.06		4.7
p	0.09 ± 0.13	0.23 ± 0.14	0.39 ± 0.24	0.38 ± 0.31	0.40 ± 0.30		2.4
$a_H(i)/a_H(m)$	0.13 ± 0.24	0.05 ± 0.20	0.35 ± 0.25	0.29 ± 0.25	0.29 ± 0.23	0.18 ± 0.09	0.04
$a_H(o)/a_H(m)$	0.64 ± 0.08	0.77 ± 0.06	0.72 ± 0.08	0.69 ± 0.08	0.80 ± 0.07	0.71 ± 0.02	0.55
$a_H(m)/a_H(m)$	1.00 ± 0.09	1.00 ± 0.07	1.00 ± 0.09	1.00 ± 0.10	1.00 ± 0.08	1.00 ± 0.03	1
$a_H(p)/a_H(m)$	0.20 ± 0.29	0.38 ± 0.23	0.52 ± 0.32	0.40 ± 0.33	0.38 ± 0.29	0.52 ± 0.05	0.51

[a] Calculated using the B3LYP/EPRII method at a M06-2X/cc-pVTZ-optimized geometry (see the Supporting Information). [b] Average over all 17 choices of n shown in Table S2 in the Supporting Information, Part C.

dx.doi.org/10.1021/ic301236s | Inorg. Chem. 2012, 51, 10819−10824

calculated average spin densities on the hydrogen atoms, $\sigma_H(\alpha)$, spin densities integrated over the four atoms of a methyl group, $\sigma_{Me}(\alpha)$, and spin densities integrated over the five atoms of a vertex, $\sigma_{RMe}(\alpha)$.

DISCUSSION

Synthesis of the isotopically labeled anions and their oxidation to radicals proceeded as expected. The only observation that requires comment is the formation of some CHD_2-substituted boron vertices upon methylation of BH vertices with $TfOCD_3$, which has mechanistic implications. Formally, it would appear that somewhere along the reaction path the system has access to structures that contain a partly rotating molecule of methane coordinated to a naked boron vertex. We have examined the reaction course computationally and shall report the results separately.

Very few polyhedral carborane radicals are known, and we are not aware of a detailed spectroscopic examination of any of them. Any system containing a spin distributed over a large number of boron atoms present in natural abundance is likely to have a density of spectral lines that will make the use of standard procedures for the extraction of values of hyperfine coupling constants difficult or impossible.

Line Width Analysis. It appears that the assumptions made in the analysis of the EPR line widths are justified because the increment method reproduces the 15 line width differences very well with only four parameters. We therefore believe that the procedure introduced here represents a useful compromise between rigor and practicality for extracting information about the coupling constants in radicals with unresolved spectra and no ENDOR signal. Admittedly, the preparation of a large number of isotopically labeled radicals was tedious, and it is possible that the system investigated presently was overdetermined excessively and unnecessarily. However, because there was little if any precedent for the procedure of analysis employed, we felt that it was important to obtain as much confidence in the consistence of the resulting values as possible. Besides, the labeled anions and radicals will also be useful for investigations of reactions in which a methyl group is transferred from the carborane cage.[24,25]

Hyperfine Coupling Constants. The information on the relative values of the hyperfine constants $a_H(\alpha)$, with $\alpha = i$, o, m, and p, that has been extracted from experiments is summarized in Table 2. It is averaged over the three hydrogen atoms in each methyl group and over all methyl groups that are equivalent by symmetry in the anion and thus does not permit us to discuss the fine details of the nature of the Jahn−Teller distortion of the radicals. It is striking that sizable coupling constants are only found in the equatorial positions meta and para (2−11), while methyl hydrogen atoms in the axial positions ipso (1) have coupling constants barely distinguishable from zero within the experimental error, and those in the other axial position para (12) are only twice as large. The coupling constants of the *m*-methyl hydrogen atoms (7−11) are about 1.5 times larger than those of the *o*-methyl hydrogen atoms (2−6).

Simple-Minded Expectations. While the coupling constants are the primary observables, spin distribution in a molecule is also of interest. Although the relationship of the spin density on the hydrogen nucleus to its coupling constants is straightforward proportionality if the Fermi contact term dominates as usual for hydrogen, the spin density on the methyl carbon atom or on the boron or carbon atom of a vertex is related to it only indirectly. In terms of a simple molecular orbital (MO) picture, an unpaired spin density is contributed primarily by the singly occupied MO (SOMO), which can be hyperconjugatively delocalized and whose amplitude on the hydrogen atom of the methyl group can then be significant. However, a similarly sized contribution can be provided by spin polarization of the bond that carries the hydrogen atom. For instance, in a planar radical with an unpaired electron in its π system, where the delocalization mechanism does not provide any spin density on a vinylic hydrogen atom by symmetry, whereas it contributes considerably to the spin density on an allylic hydrogen atom, the coupling constants of the two types of hydrogen atoms are comparable.[27,28] Similar analyses of the interplay of spin delocalization and spin polarization have been performed in some saturated radicals[29] but, to our knowledge, not for substituents on a carborane cage.

In the absence of Jahn−Teller distortion, the SOMO of **1** is a cage orbital with three nodal planes that share the 5-fold symmetry axis and has zero amplitude in the ipso and para positions (1 and 12, respectively).[12] The distribution of this MO over the molecule provides an initial clue to the spin distribution in the radical. The amplitudes calculated for the ortho and meta positions (2−6 and 7−11, respectively) are large and comparable. Qualitatively, at the symmetric geometry, one would not expect either the delocalization or polarization mechanism to contribute much in the axial positions because neither the cage atoms 1 and 12 nor their methyl carbon atoms can participate significantly in the SOMO (the first atomic orbitals of symmetry appropriate for participation are 4f). Symmetry does not prevent the methyl hydrogen atoms from participating, but there is no connecting path for either the delocalization or polarization mechanism. This result agrees perfectly with the observed small coupling constants of the methyl hydrogen atoms in the axial positions 1 and 12 but does not explain why the coupling constant is twice as large in the latter position.

The large coupling constants on the methyl groups in the equatorial positions 2−11 do not come as a surprise either. Because the SOMO has large amplitudes on the vertex boron atoms, primarily on their horizontal tangential 2p atomic orbitals, one can expect spin delocalization on the methyl carbon and hydrogen atoms by hyperconjugation, especially on the hydrogen atom whose CH bond is close to parallel to the equatorial plane. The spin polarization mechanism may contribute as well, but if the situation is similar to that known from π systems, it will not be dominant. The significant difference between the ortho (2−6) and meta (7−11) positions is not foreseen by this simple analysis. It is not predicted by a simple consideration of the shape of the SOMO, and it is not obvious why spin polarization of the bonds should be different in the two types of position.

In the presence of the Jahn−Teller distortion, the symmetry is lowered. The geometry optimization for radical **1r** yielded only one minimum, whereas for the unsubstituted parent $CB_{11}H_{12}^{\bullet}$, two minima differing in the nature of the Jahn−Teller distortion were found.[12] Now, the three nodal planes no longer pass exactly through the vertices 1 and 12 and the atoms attached to them. This apparently has a very small effect in position 1 but more in position 12.

Comparison with Density Functional Theory (DFT) Calculations. The coupling constant ratios shown in Table 2 are in quite good agreement with the simple analysis and with the experimental results. The ratios of the $a_H(\alpha)$ values at the *i*, *o*, *m*, and *p* vertices of the radical **1r** are (0.18 ± 0.09):(0.71 ±

0.02):(1.00 ± 0.03):(0.52 ± 0.05) from experiment and 0.04:0.55:1:0.51 from calculation, in respectable agreement within the experimenal error, given the presumably complicated dynamic Jahn−Teller effect in the radical (note that the 12-fold calculated difference between the *i* and *p* positions is only 3-fold in reality). Even the ratios of calculated spin densities $\sigma_H(\alpha)$, $\sigma_{Me}(\alpha)$, and $\sigma_{BMe}(\alpha)$ are fairly similar, that is, 0.01:0.60:1:0.09, 0.01:0.53:1:0.06, and −0.01:0.51:1:0.10, except that the observed and computed values of $a_H(p)$ are disproportionately large considering the spin densities. It appears that in the para position spin polarization makes a larger contribution to the coupling constant than in the other positions.

All of these ratios are distinctly different from those of the incremental contributions to the increase of the potential of the **1**/**1r** redox couple as a methyl substituent in the same position is removed and replaced by a hydrogen atom, 0.43^{14}:0.97^{12}:1^{12}:$0.97.^{14}$ In the first approximation, one might have expected more similarity, because when the Jahn−Teller distortion is ignored, first-order perturbation theory would suggest that both types of quantities are related to the same squares of the amplitudes of the highest occupied MO (HOMO) of **1** or the SOMO of **1r** at the vertex in question (adding contributions from both degenerate components in the anion). The situation is clearly more complicated than a first glance suggests and leads us to suspect that the relative simplicity observed for planar π-electron systems should not be expected in the three-dimensionally conjugated carboranes.

SUMMARY

The line widths in the EPR spectra of the 16 radicals **1r**−**16r** have been determined and analyzed in terms of a simple model that derives the ratios of the four hyperfine coupling constants associated with methyl hydrogen atoms in the four symmetrically inequivalent positions of substitution. These ratios are in qualitative agreement with values calculated by DFT and distinctly different from the ratios of increments that describe the effects of methyl substitution on the reversible oxidation potentials of the corresponding anions, altough simple arguments suggest that both should be directly related to the distribution of the anion HOMO over the molecule.

ASSOCIATED CONTENT

Supporting Information

Part A describing the detailed synthetic procedures for the anions **1**−**56**, part B containing the ^{1}H, ^{2}H, ^{13}C, and ^{11}B NMR and ESI mass spectra of the anions **1**−**16**, and part C describing the EPR measurement and evaluation procedures and computational methods. This material is available free of charge via the Internet at http://pubs.acs.org.

AUTHOR INFORMATION

Corresponding Author

*E-mail: michl@eefus.colorado.edu.

Notes

The authors declare no competing financial interest.

ACKNOWLEDGMENTS

This material is based upon work supported by the Academy of Sciences of the Czech Republic (Grant M200550906), Grant Agency of the Czech Republic (Grant 203/09/J058), Institute of Organic Chemistry and Biochemistry (RVO: 61388963 and 820/82), and the U.S. NSF (Grant CHE0848477). We are grateful to Prof. Raul Crespo (University of Valencia) for providing the optimized geometry of the $CB_{11}Me_{12}^{\bullet}$ radical.

REFERENCES

(1) Grimes, R. N. *Carboranes*, 2nd ed.; Elsevier: Amsterdam, The Netherlands, 2011.
(2) Körbe, S.; Schreiber, P. J.; Michl, J. *Chem. Rev.* **2006**, *106*, 5208.
(3) Reed, C. A. *Acc. Chem. Res.* **1998**, *31*, 133.
(4) Reed, C. A. *Acc. Chem. Res.* **2009**, *43*, 121.
(5) King, B.; Michl, J. *J. Am. Chem. Soc.* **2000**, *122*, 10255.
(6) Lipping, L.; Leito, I.; Koppel, I.; Koppel, I. A. *J. Phys. Chem. A* **2009**, *113*, 12972.
(7) Hoffmann, S.; Juhasz, M.; Reed, C. *J. Am. Chem. Soc.* **2006**, *128*, 3160.
(8) Moss, S.; King, B. T.; de Meijere, A.; Kozhushkov, S. I.; Eaton, P. E.; Michl, J. *Org. Lett.* **2001**, *3*, 2375.
(9) Volkis, V.; Mei, H.; Shoemaker, R. K.; Michl, J. *J. Am. Chem. Soc.* **2009**, *131*, 3132.
(10) King, B. T.; Janoušek, Z.; Grüner, B.; Trammel, M.; Noll, B. C.; Michl, J. *J. Am. Chem. Soc.* **1996**, *118*, 3313.
(11) King, B. T.; Noll, B. C.; McKinley, A. J.; Michl, J. *J. Am. Chem. Soc.* **1996**, *118*, 10902.
(12) King, B. T.; Körbe, S.; Schreiber, P. J.; Clayton, J.; Němcová, A.; Havlas, Z.; Vyakaranam, K.; Fete, M. G.; Zharov, I.; Ceremuga, J.; Michl, J. *J. Am. Chem. Soc.* **2007**, *129*, 12960.
(13) Fete, M. G.; Havlas, Z.; Michl, J. *J. Am. Chem. Soc.* **2011**, *133*, 4123.
(14) Wahab, A.; Stepp, B. R.; Douvris, C.; Valášek, M.; Štursa, J.; Klíma, J.; Piqueras, M.-C.; Crespo, R.; Ludvík, J.; Michl, J. *Inorg. Chem.* **2012**, *51*, 5128.
(15) Wiersema, R. J.; Hawthorne, M. F. *Inorg. Chem.* **1973**, *12*, 785.
(16) Hawthorne, M. F.; Pilling, R. L.; Stokely, P. F. *J. Am. Chem. Soc.* **1965**, *87*, 1893.
(17) Watson-Clark, R. A.; Knobler, C. B.; Hawthorne, M. F. *Inorg. Chem.* **1996**, *35*, 2963.
(18) Middaugh, R. L.; Farha, F., Jr. *J. Am. Chem. Soc.* **1966**, *88*, 4147.
(19) Wiersema, R. J.; Middaugh, R. L. *J. Am. Chem. Soc.* **1967**, *89*, 5078.
(20) Hawthorne, M. F.; Shelly, K.; Li, F. *Chem. Commun.* **2002**, 547.
(21) Zharov, I.; King, B. T.; Havlas, Z.; Pardi, A.; Michl, J. *J. Am. Chem. Soc.* **2000**, *122*, 10253.
(22) Zharov, I.; Weng, T.; Orendt, A. M.; Barich, D. H.; Penner-Hahn, J.; Grant, D. M.; Havlas, Z.; Michl, J. *J. Am. Chem. Soc.* **2004**, *126*, 12033.
(23) Zharov, I.; Havlas, Z.; Orendt, A. M.; Barich, D. H.; Grant, D. M.; Fete, M. G.; Michl, J. *J. Am. Chem. Soc.* **2006**, *128*, 6089.
(24) Volkis, V.; Douvris, C.; Michl, J. *J. Am. Chem. Soc.* **2011**, *133*, 7801.
(25) Janoušek, Z.; Lehmann, U.; Častulík, J.; Císařová, I.; Michl, J. *J. Am. Chem. Soc.* **2004**, *126*, 4060.
(26) Valášek, M.; Štursa, J.; Pohl, R.; Michl, J. *Inorg. Chem.* **2010**, *49*, 10255.
(27) Weil, J. A.; Bolton, J. R.; Wertz, J. E. *Electron Paramagnetic Resonance: Elementary Theory and Practical Applications*; Wiley: New York, 1994.
(28) Carrington, A.; McLachlan, A. D. *Introduction to Magnetic Resonance*, 3rd ed.; Chapman and Hall: London, 1979.
(29) McKinley, A. J.; Ibrahim, P. N.; Balaji, V.; Michl, J. *J. Am. Chem. Soc.* **1992**, *114*, 10631.